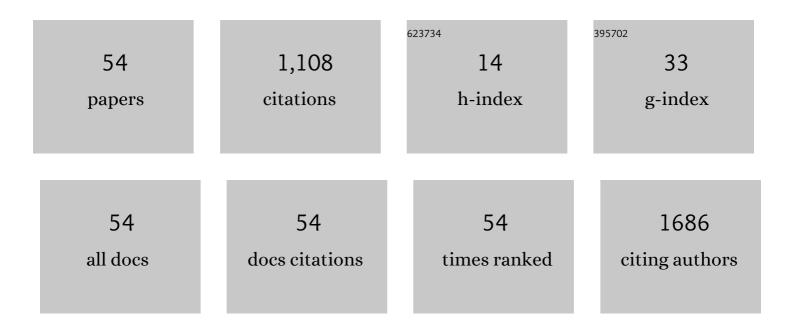
## Yelong Wu

## List of Publications by Year in descending order

Source: https://exaly.com/author-pdf/4412342/publications.pdf Version: 2024-02-01



YELONG WU

#	Article	IF	CITATIONS
1	Grain-Boundary-Enhanced Carrier Collection in CdTe Solar Cells. Physical Review Letters, 2014, 112, 156103.	7.8	258
2	Engineering Grain Boundaries in Cu <sub>2</sub> ZnSnSe <sub>4</sub> for Better Cell Performance: A Firstâ€Principle Study. Advanced Energy Materials, 2014, 4, 1300712.	19.5	135
3	From atomic structure to photovoltaic properties in CdTe solar cells. Ultramicroscopy, 2013, 134, 113-125.	1.9	80
4	Sulfur dioxide adsorbed on graphene and heteroatom-doped graphene: a first-principles study. European Physical Journal B, 2013, 86, 1.	1.5	79
5	Physics of grain boundaries in polycrystalline photovoltaic semiconductors. Journal of Applied Physics, 2015, 117, .	2.5	52
6	Carrier Separation at Dislocation Pairs in CdTe. Physical Review Letters, 2013, 111, 096403.	7.8	51
7	Defect segregation at grain boundary and its impact on photovoltaic performance of CuInSe2. Applied Physics Letters, 2013, 102, .	3.3	50
8	Sulfur dioxide molecule sensors based on zigzag graphene nanoribbons with and without Cr dopant. Physics Letters, Section A: General, Atomic and Solid State Physics, 2014, 378, 667-671.	2.1	38
9	LDA+U/GGA+U calculations of structural and electronic properties of CdTe: Dependence on the effective U parameter. Computational Materials Science, 2015, 98, 18-23. Adsorption behavior of formaldehyde on ZnO <mml:math< td=""><td>3.0</td><td>25</td></mml:math<>	3.0	25
10	xmlns:mml="http://www.w3.org/1998/Math/MathML" altimg="si8.gif" overflow="scroll"> < mml:mrow > < mml:mrow > < mml:mo		

Yelong Wu

#	Article	IF	CITATIONS
19	Electronic properties of MoS <sub>2</sub> sandwiched between graphene monolayers. Europhysics Letters, 2014, 106, 47003.	2.0	12
20	Tailoring the surface of ZnO nanorods into corrugated nanorods via a selective chemical etch method. Nanotechnology, 2016, 27, 295601.	2.6	12
21	Unusual nonlinear strain dependence of valence-band splitting in ZnO. Physical Review B, 2012, 86, .	3.2	11
22	The structure and properties of (aluminum, oxygen) defect complexes in silicon. Journal of Applied Physics, 2013, 114, 063520.	2.5	10
23	Interaction between phosphorene and the surface of a substrate. Materials Research Express, 2016, 3, 025013.	1.6	10
24	Crystallography facet tailoring of carbon doped ZnO nanorods via selective etching. Applied Surface Science, 2017, 406, 186-191.	6.1	10
25	Spontaneous polarization and piezoelectric properties of AlN nanowires: Maximally localized Wannier functions analysis. Europhysics Letters, 2015, 111, 67003.	2.0	9
26	Hybrid-functional calculations of electronic structure and phase stability of MO (M = Zn, Cd, Be, Mg,) Tj ETQq0 C 8507-8514.	0 rgBT /0 3.6	verlock 10 Tf 9
27	Electronic and structural properties of N-vacancy in AlN nanowires: A first-principles study. Chinese Physics B, 2012, 21, 087101.	1.4	8
28	First-principles study on native point defects of cubic cuprite Ag2O. Journal of Applied Physics, 2016, 120, .	2.5	8
29	Water adsorption behaviors of high index polar surfaces in ZnO. Applied Surface Science, 2019, 498, 143898.	6.1	8
30	From the absolute surface energy to the stabilization mechanism of high index polar surface in wurtzite structure: The case of ZnO. Journal of Alloys and Compounds, 2019, 772, 482-488.	5.5	8
31	Crystal structure and photoluminescence properties of blue-green-emitting Ca1â^'xSrxZr4(PO4)6: Eu2+ (0â‰æâ‰⊉) phosphors. Materials Research Bulletin, 2020, 125, 110781.	5.2	8
32	Double perovskite Ba2BiTaO6 as a promising <i>p</i> -type transparent conductive oxide: A first-principles defect study. Journal of Applied Physics, 2020, 127, .	2.5	7
33	Origin of charge separation in III-nitride nanowires under strain. Applied Physics Letters, 2011, 99, 262103.	3.3	6
34	Column-by-column observation of dislocation motion in CdTe: Dynamic scanning transmission electron microscopy. Applied Physics Letters, 2016, 109, .	3.3	6
35	A novel laser scribing method combined with the thermal stress cleaving for the crystalline silicon solar cell separation in mass production. Solar Energy Materials and Solar Cells, 2022, 240, 111714.	6.2	6
36	Nanoporous AlN particle production from a solid-state metathesis reaction. Chinese Physics B, 2009, 18, 2925-2927.	1.4	5

Yelong Wu

#	Article	IF	CITATIONS
37	Theoretical study of the stabilization mechanisms of the different stable oxygen incorporated (101Â <sup>-</sup> 0) surface of III-nitrides. Journal of Applied Physics, 2010, 107, 043529.	2.5	4
38	Ternary mixed crystal effects on interface optical phonon and electron-phonon coupling in zinc-blende GaN/AlxGa1â^'xN spherical quantum dots. Physica E: Low-Dimensional Systems and Nanostructures, 2016, 76, 164-168.	2.7	4
39	Preparations of porous AlN particles from an aluminum–magnesium alloy melt solution. Materials Letters, 2009, 63, 2205-2207.	2.6	3
40	Optimization Design of a Multibusbar Structure: The Using of a Conductive Belt. International Journal of Photoenergy, 2018, 2018, 1-12.	2.5	3
41	The stabilization mechanism and size effect of nonpolar-to-polar crystallography facet tailored ZnO nano/micro rods <i>via</i> a top-down strategy. Physical Chemistry Chemical Physics, 2018, 20, 18455-18462.	2.8	3
42	Structural and optical properties of porous ZnO nanorods synthesized by a simple two-step method. Superlattices and Microstructures, 2019, 128, 30-36.	3.1	3
43	Electronic properties and stability of M <sub>2</sub> O <sub>3</sub> (MÂ=ÂAl, Ga, In) and alloy (M <sub>x</sub> Ga <sub>1â€x</sub> ) <sub>2</sub> O <sub>3</sub> in α and β phases: A theoretical study. Journal of the American Ceramic Society, 2022, 105, 4554-4563.	3.8	3
44	Photoluminescence Properties and Energy Transfers in the Novel LiYMgWO <sub>6</sub> : Dy <sup>3+</sup> , Tm <sup>3+</sup> . , 2022, 1, 025001.		3
45	A novel anion interstitial defect structure in zinc-blende materials: A first-principles study. Europhysics Letters, 2016, 114, 36001.	2.0	2
46	Understanding Individual Defects in CdTe Solar Cells: From Atomic Structure to Electrical Activity. Microscopy and Microanalysis, 2014, 20, 518-519.	0.4	1
47	Column-by-Column Imaging of Dislocation Slip Processes in CdTe. Microscopy and Microanalysis, 2014, 20, 1054-1055.	0.4	1
48	Effect of oxygen vacancy and zinc interstitial on the spontaneous polarization of wurtzite ZnO: maximally localized Wannier functions analysis. EPJ Applied Physics, 2015, 70, 20101.	0.7	1
49	First-Principles Investigation of Electronic Structure and Energy Level Scheme of Phosphors: The Lanthanide-Doped Sr2P2O7. ECS Journal of Solid State Science and Technology, 0, , .	1.8	1
50	Defect levels in d-electron containing systems: Comparative study of CdTe using LDA and LDA + U. Journal of Semiconductors, 2020, 41, 102701.	3.7	1
51	Hole-Induced Spontaneous Mutual Annihilation of Dislocation Pairs. Journal of Physical Chemistry Letters, 2019, 10, 7421-7425.	4.6	0
52	Polarization properties of AlN (101ì0) and (112ì0) non-polar surfaces: maximally localized Wannier functions study. EPJ Applied Physics, 2019, 88, 10101.	0.7	0
53	Influence of vacancy on spontaneous polarization of wurtzite AlN: a maximally localized Wannierfunction study. Wuli Xuebao/Acta Physica Sinica, 2014, 63, 167701.	0.5	0
54	Absolute surface energies of wurtzite (10 1Â⁻1) surfaces and the instability of the cation-adsorbed surfaces of II–VI semiconductors. Applied Physics Letters, 2021, 119, 201603.	3.3	0